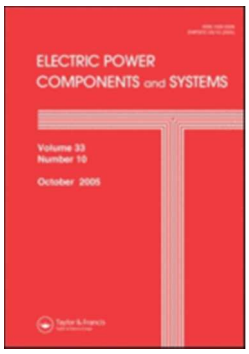

Study of resonances in 1x25kV AC traction systems

Journal:	*Electric Power Components and Systems*
Manuscript ID:	Draft
Manuscript Type:	Original Article
Date Submitted by the Author:	n/a
Complete List of Authors:	Monjo, Lluis; Universitat Politècnica de Catalunya, Electrical Engineering Sainz, Luis; Universitat Politècnica de Catalunya,
Keywords:	harmonics, resonances, power quality

Study of resonances in 1x25kV AC traction systems

Ll. Monjo and L. Sainz

Department of Electrical Engineering, ETSEIB-UPC, Av. Diagonal 647, Barcelona 08028, Spain.
E-mails: lluis.monjo@upc.edu, sainz@ee.upc.edu

Abstract: AC traction systems are 1x25 or 2x25 kV 50 Hz single-phase, non-linear, time-varying loads that can cause power quality problems. One of the main concerns about these systems is voltage distortion because adjustable speed drives for trains may inject harmonic currents of frequencies below 2 kHz. Since the presence of parallel resonances in the contact feeder section of the traction circuit worsens the scenario, traction system resonance phenomena should be analyzed to prevent problems. Several works address these phenomena but they only draw weak numerical conclusions based on the frequency scan method. This paper studies 1x25 kV traction system resonances at pantograph terminals and provides more effective analytical expressions to locate them and determine the impact of traction system parameters on them. These expressions are validated from several traction systems in the literature.

Keywords: Harmonic analysis, resonance, traction systems, power quality

1 Introduction

Although 2x25 kV traction systems are common in high-speed railways because of their ability to meet high power requirements with lower currents at the contact feeder section, 1x25 kV traction systems are still operating in traditional and high-speed railways [1] – [6]. The main concerns about these systems are related to power quality because traction loads are single-phase, non-linear, time-varying loads closely connected to the utility power supply system [7] – [10]. In particular, special attention must be paid to the presence of harmonics [1], [9] – [12]. Many distorting sources in traction systems inject harmonics into transformer substations and traction lines, with the main being adjustable speed drives for trains [1], [7]. Although pulse-width-modulated (PWM) drives with nearly unity power factor and reduced harmonic current content are the most widely used in modern locomotives, the harmonic problem remains important because of the wide range of frequencies of

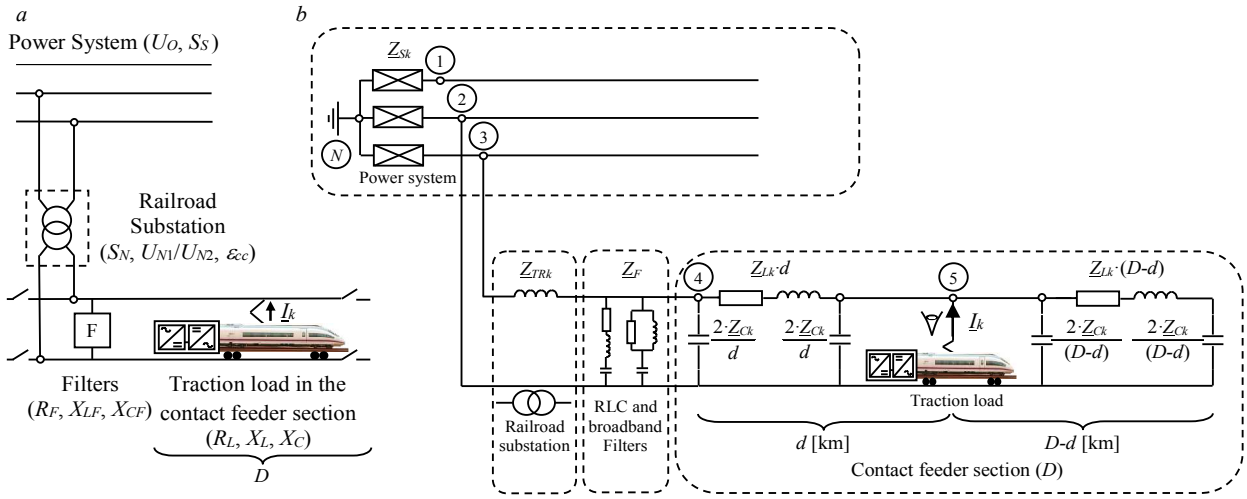

Fig. 1 *1x25kV AC traction system*
a Railroad substation connection scheme
b Harmonic equivalent impedance circuit of the system

injected currents (especially, the 1 to 2 kHz range close to the converter switching frequency) [2], [7], [10], [11]. The problem is worse in trains equipped with phase-controlled thyristor converters because they consume currents with a low displacement power factor and high frequency content (in particular, frequencies below 450 Hz) [4], [11] – [13]. Moreover, the use of converters with advanced control characteristics and new signaling systems requires a higher power quality level to avoid electromagnetic interference in power and signaling devices [1], [7], which can strongly affect system safety and reliability [11].

The harmonic problem is worsened with the presence of resonances in the contact feeder section of the traction circuit, because they can increase harmonic voltage distortion. Thus, many works have addressed the resonance problem at traction system pantograph terminals experimentally and numerically [1] – [3], [7], [10], [14] – [16]. In [2], [3], [10], [15], resonance is analyzed from

Table 1 *1x25kV 50 Hz traction system data and ratios [2], [3], [5], [15], [18]*

			System data	System ratios	
Power System	Open-circuit voltage	U_o	220, 132 kV		
	Short-circuit power	S_s	> 700MVA	x_S (pu)	< 0.143
Substation transformer	Transformer ratio	U_{N1}/U_{N2}	220 - 132/25 kV		
	Rated power	S_N	12, 30 MVA		
	Short-circuit Impedance	ε_{cc}	≈ 5 … 12 %		
Contact feeder section	Longitudinal PI resistance	R_L	0.0125 ... 1.3125 Ω/km	r_L (pu/km)	0.002 ... 0.21
	Longitudinal PI reactance	X_L	0.0625 ... 2.1875 Ω/km	x_L (pu/km)	0.01 ... 0.35
	Transversal PI reactance	X_C	$1.2497\cdot10^5$ ... $1.5642\cdot10^6$ Ω·km	x_C (pu·km)	$2.0\cdot10^4$ ... $2.5\cdot10^5$
	Track length	D	30, 40 km		

Note:
- The RLC and broadband filter parameters depend on the reactive power consumption of the traction system and filter tuning frequency.
- The system ratios are calculated from the following values of the traction system parameters:
  - Power system: U_O = 220 kV
  - Substation transformer: S_N = 12 MVA, ε_{cc} = 12 % (i.e., X_{TR} = 6.25 Ω)

measurements and, in [1], [2], [7], [10], [14] – [16], it is studied from simulations considering line distributed models to determine the influence of the position of the train on the track. These works only report examples about traction system resonance frequencies obtained by the frequency scan method but do not analyze resonances in depth or provide analytical expressions for their location. They conclude that resonances are in the range of 1 to 20 kHz, and pay some more attention to the lowest resonance (close to the 1 to 2 kHz switching frequency of PWM drive converters) by briefly analyzing the influence of system parameters on it. From the frequency scan study, most works deduce that the lowest resonance mainly depends on the substation reactance and the capacitance between the contact wire and the ground, rather than on the train position on the track. However, none points out or analyzes the limitation of this assertion [2], [4], [7], [14], [15]. Thus, the main challenge is to provide analytical expressions which are more accurate and useful than frequency scan plots in understanding and predicting resonance phenomena. In order to reduce harmonic currents injected into networks and mitigate resonances, active and hybrid systems can be used in locomotives, and RLC and broadband passive filters in traction systems. These filters are often linked with the fundamental reactive power compensation goal. Because several different types of locomotives run simultaneously on the same traction section, placing passive filters at the 25 kV side of the traction substation is usually the most effective and economical mitigation technique [3], [8], [11], [13], [15], [16] and [17]. Most previous works study unfiltered traction systems to determine the extent of the harmonic problem, and subsequently analyze how filters alleviate the resonance problem and plan their connection.

From the framework in [18], the present paper provides analytical expressions for locating all the resonance frequencies observed from the traction load at pantograph terminals in unfiltered 1x25 kV railway power systems. These expressions make it possible to investigate 1x25 kV railway power system resonances in more detail than frequency scan plots. Moreover, the influence of traction system parameters and train position on resonance is determined. The expressions are validated with several traction systems in the literature where resonances are numerically and experimentally located.

2 1x25 kV supply of AC traction systems

Many electrified traction systems operate on 1x25kV 50Hz. In these systems, traction loads are supplied by a single-phase overhead contact line distributed in different sections along the line. These sections, usually of lengths (D) 30 or 40 km [3], [5], [12], [14] – [16], are connected through a transformer to the main power network, Fig. 1(a). For steady-state studies, railway traction systems are modeled with their equivalent circuit, which is formed by

- The power system: It is characterized from its open-circuit voltage U_O and short-circuit power S_S at the point of coupling.
- The railroad substation U_{N1}/U_{N2} transformer: It is characterized from its rated power S_N and per-unit short-circuit impedance ε_{cc}.

- The RLC and broadband filters: They are characterized from their filter component impedances (X_{CF}, X_{LF} and R_F) [17].
- The contact feeder section: It is represented by its equivalent impedance circuit characterized by a distributed model dependent on train position with two π-sections at the left and right side of the traction load [3], [14], [15]. The per-unit-length longitudinal impedance of the line (i.e., R_L and X_L) and the per-unit-length parallel impedance between the line and the ground (i.e., X_C) are considered in both sections.

The usual values of the above parameters are in Table 1.

In electrified traction systems, electric traction locomotives fed by adjustable speed drives are a source of harmonic currents $\underline{I}_k$ [2], [4], [7], [10] – [13]. These may distort voltages, affecting power quality. This problem is aggravated by the presence of resonances in the system equivalent impedances of the contact feeder section [2], [3], [5], [7], [12]. To avoid this, many works locate resonances at pantograph terminals of unfiltered traction systems by the frequency scan method, yet this technique provides little information about the problem. This is why analytical expressions would be useful to have a full picture of the problem. Traction system harmonic behavior is analyzed and analytical expressions to locate resonances are provided in the next Sections.

3 Traction system harmonic analysis

The harmonic behavior of the passive set "observed" from the traction load is studied to locate resonances. As can be seen in Fig. 1(b), this set is formed by the impedances (or admittances) of the power system, the railroad substation transformer, the passive filters and the contact feeder section [3], [13], [15], [16], [17]:

- Power system admittance: It includes the impedance of the power supply and the short-circuit impedance of the three-phase transformer feeding the traction system:

$$\underline{Y}_{Sk} = \underline{Z}_{Sk}^{-1} \approx \frac{1}{jkX_S} = \left(jk \frac{U_O^2}{S_S} \left(\frac{U_{N2}}{U_{N1}} \right)^2 \right)^{-1} . \quad (1)$$

- Railroad substation transformer admittance: It represents the short-circuit impedance of the transformer feeding the contact feeder section:

$$\underline{Y}_{TRk} = \underline{Z}_{TRk}^{-1} \approx \frac{1}{jkX_{TR}} = \left(jk\varepsilon_{cc} \frac{U_{N2}^2}{S_N} \right)^{-1} . \quad (2)$$

- RLC and broadband filter admittances: They represent the RLC and broadband filter impedances ($\underline{Z}_{Fk}$ and $\underline{Z}_{Fbk}$, respectively):

$$\underline{Y}_{Fk} = \underline{Z}_{Fk}^{-1} = \frac{1}{R_F + j(kX_{LF} - X_{LF}/k)} \qquad \underline{Y}_{Fbk} = \underline{Z}_{Fbk}^{-1} = \left(\frac{R_F \cdot jkX_{LFb}}{R_F + jkX_{LFb}} - j\frac{X_{CFb}}{k} \right)^{-1} . \quad (3)$$

- Contact feeder section admittances: They represent the per-unit-length longitudinal and transversal

impedances of the catenary lines:

$$\underline{Y}_{Lk} = \underline{Z}_{Lk}^{-1} = \frac{1}{R_L + jkX_L} \qquad \underline{Y}_{Ck} = \underline{Z}_{Ck}^{-1} = j\frac{k}{X_C}. \tag{4}$$

The resistances of the power system and substation transformer impedances (i.e., R_S and R_{TR}, respectively) are neglected in this study because it is well-known that they damp the system harmonic response but do not affect resonance location significantly [18].

By considering point N in Fig. 1(b) as the reference bus, the harmonic behavior of the system can be characterized by the admittance matrix,

$$\begin{bmatrix} \underline{V}_{1k} \\ \vdots \\ \underline{V}_{5k} \end{bmatrix} = \begin{bmatrix} \underline{Z}_{11k} & \cdots & \underline{Z}_{15k} \\ \vdots & \ddots & \vdots \\ \underline{Z}_{51k} & \cdots & \underline{Z}_{55k} \end{bmatrix} \begin{bmatrix} 0 \\ \vdots \\ \underline{I}_k \end{bmatrix} = \begin{bmatrix} \underline{Y}_{Sk} & 0 & 0 & 0 & 0 \\ 0 & \underline{Y}_{22k} & 0 & -\underline{Y}_{24k} & -\underline{Y}_{25k} \\ 0 & 0 & \underline{Y}_{33k} & -\underline{Y}_{TRk} & 0 \\ 0 & -\underline{Y}_{24k} & -\underline{Y}_{TRk} & \underline{Y}_{44k} & -\underline{Y}_{Lk}/d \\ 0 & -\underline{Y}_{25k} & 0 & -\underline{Y}_{Lk}/d & \underline{Y}_{55k} \end{bmatrix}^{-1} \begin{bmatrix} 0 \\ 0 \\ 0 \\ 0 \\ \underline{I}_k \end{bmatrix}, \tag{5}$$

where

$$\begin{aligned} \underline{Y}_{22k} &= \underline{Y}_{Sk} + d\underline{Y}_{Ck} + \frac{(D-d)\underline{Y}_{Ck}}{2} + \underline{Y}_{s2k} + \underline{Y}_{Fk} + \underline{Y}_{Fbk} & \underline{Y}_{33k} &= \underline{Y}_{Sk} + \underline{Y}_{TRk} \\ \underline{Y}_{44k} &= \underline{Y}_{TRk} + \frac{d\underline{Y}_{Ck}}{2} + \frac{\underline{Y}_{Lk}}{d} + \underline{Y}_{Fk} + \underline{Y}_{Fbk} & \underline{Y}_{55k} &= \frac{d\underline{Y}_{Ck}}{2} + \frac{\underline{Y}_{Lk}}{d} + \frac{(D-d)\underline{Y}_{Ck}}{2} + \underline{Y}_{s2k} \\ \underline{Y}_{24k} &= \frac{d\underline{Y}_{Ck}}{2} + \underline{Y}_{Fk} + \underline{Y}_{Fbk} & \underline{Y}_{25k} &= \frac{d\underline{Y}_{Ck}}{2} + \frac{(D-d)\underline{Y}_{Ck}}{2} + \underline{Y}_{s2k} \\ \underline{Y}_{s2k} &= \frac{(\underline{Y}_{Lk}\underline{Y}_{Ck}/2)}{(\underline{Y}_{Lk}/(D-d) + (D-d)\underline{Y}_{Ck}/2)}, \end{aligned} \tag{6}$$

and d is the train position along the contact feeder section. From (5), the equivalent harmonic impedance, which relates the k^{th} harmonic current and voltage at the pantograph node (i.e., at node 5 in Fig. 1(b)), can be obtained as follows:

$$\underline{V}_{5k} - \underline{V}_{2k} = (\underline{Z}_{55k} + \underline{Z}_{22k} - 2\underline{Z}_{25k})\underline{I}_k = \underline{Z}_{Eqk}\underline{I}_k. \tag{7}$$

The analysis of this impedance in a frequency range makes it possible to locate the resonances observed from the traction load. As an example, Fig. 2 shows the frequency response of the unfiltered

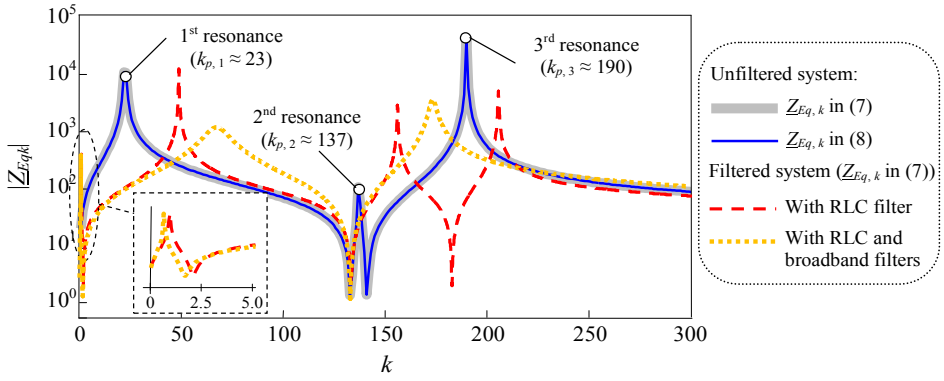

Fig. 2 *Frequency response of the system equivalent impedance observed from the traction load when it is located at d = D/2 with D = 30 km.*

and filtered system equivalent impedance numerically obtained from (5) and (7) considering the train position $d = D/2$ with $D = 30$ km and the impedance values $X_s = 0.6944\ \Omega$ ($S_S = 900$ MVA), $X_{TR} = 6.25\ \Omega$ ($S_N = 12$ MVA and $\varepsilon_{cc} = 12\ \%$), $R_L = 0.0232\ \Omega$/km, $X_L = 0.0625\ \Omega$/km and $X_C = 1.25 \cdot 10^5\ \Omega \cdot$km. Track length and impedance values are obtained from the usual traction system parameters in Table 1. Two cases are considered in the filtered system: (*i*) An RLC filter tuned at the 3rd harmonic and (*ii*) a combination of an RLC filter and a broadband filter tuned at the 3rd and 5th harmonics, respectively. The unfiltered system impedance in Fig. 2 (solid gray line) has the typical parallel resonances in the literature, and only the first at $k_{p,1} \approx 23$ (i.e., $f_{p,1} \approx 1.2$ kHz) can be problematic due to its proximity to the switching frequency of train converters [2], [3], [7], [10], [11], [14], [15]. The filters allow shifting the parallel resonances to higher frequencies and damping their magnitude, thereby reducing the harmonic problem.

The unfiltered system impedance is analytically determined and simple expressions to locate resonances are obtained in the following Section. This makes it possible to predict the harmonic problem and design shunt filters to avoid it.

4 Analytical characterization of the traction system harmonic response

4.1 Traction system harmonic impedance

Impedance $\underline{Z}_{Eqk}$ is obtained from (5) and (7) without considering the filters and is normalized with respect to the substation transformer reactance to reduce the number of variables in the study:

$$\underline{Z}_{Eqk,N} = \frac{\underline{Z}_{Eqk}}{X_{TR}} = \frac{1}{X_{TR}} \left(\frac{\underline{Y}_{Ck}(D-d)\left(4\underline{Y}_{Lk} + (D-d)^2\,\underline{Y}_{Ck}\right)}{2\left(2\underline{Y}_{Lk} + (D-d)^2\,\underline{Y}_{Ck}\right)} + \frac{2\underline{Y}_{Pk}\underline{Y}_{Lk} + d \cdot \underline{Y}_{Ck}(d \cdot \underline{Y}_{Pk} + \underline{Y}_{Lk})}{2(d \cdot \underline{Y}_{Pk} + \underline{Y}_{Lk})} \right)^{-1}, \tag{8}$$

where

$$\underline{Y}_{Pk} = \frac{\underline{Y}_{Sk}\underline{Y}_{TRk}}{\underline{Y}_{Sk} + 2\underline{Y}_{TRk}} + \frac{d}{2}\underline{Y}_{Ck}. \tag{9}$$

Expression (8) can also be obtained directly by simple inspection of the circuit in Fig. 1(b).

To validate the analytical expression of $\underline{Z}_{Eqk,N}$ in (8), Fig. 2 compares its frequency response (shown by a dashed black line) with that calculated in Section 3. It is verified that the accuracy obtained can be extended to any value of the system parameters in Table 1.

It is easy to demonstrate that the normalized impedance $\underline{Z}_{Eqk,N}$ only depends on the following terms:

$$\begin{aligned} X_{TR}\underline{Y}_{Sk} &\approx \frac{X_{TR}}{jkX_S} = \frac{1}{jkx_S} & X_{TR}\underline{Y}_{TRk} &\approx \frac{X_{TR}}{jkX_{TR}} = \frac{1}{jk} \\ X_{TR}\underline{Y}_{Lk} &= \frac{X_{TR}}{R_L + jkX_L} = \frac{1}{r_L + jkx_L} & X_{TR}\underline{Y}_{Ck} &= j\frac{kX_{TR}}{X_C} = j\frac{k}{x_C}, \end{aligned} \tag{10}$$

and therefore the magnitude of the normalized impedance $\underline{Z}_{Eqk,N}$ only depends on the harmonic order

k, track length D, train position d and four ratios $x_S = X_S/X_{TR}$, $r_L = R_L/X_{TR}$, $x_L = X_L/X_{TR}$ and $x_C = X_C/X_{TR}$. Table 1 shows typical values of these ratios derived from the traction system parameter data. In the next subsection, simple expressions to locate the resonances of $\underline{Z}_{Eqk,N}$ (or $\underline{Z}_{Eqk}$) based on the previous variables are determined.

4.2 Analytical location of resonance

The resonances of $\underline{Z}_{Eqk,N}$ can be analytically located from (8) by equating to zero its denominator, which can be compacted as follows:

$$\mathrm{Den}\left(\underline{Z}_{Eqk,N}\right) = k^6 c_3 + k^4 c_2 + k^2 c_1 + c_0, \tag{11}$$

where the coefficients of the equations are

$$\begin{aligned} c_3 &= x_L^2 D \cdot d^2 \cdot (D-d)^2 \left(1 + 2x_S\right) \\ c_2 &= -2x_C x_L D \cdot \left(\left(D^2 - D \cdot d + d^2\right) + x_L d \cdot \left(D-d\right)^2\right) + 4x_S x_L x_C D \cdot \left(D^2 - D \cdot d + d^2\right) \\ c_1 &= 4x_C^2 D \cdot \left(\left(2 + D \cdot x_L\right) + 4x_S\right) \qquad c_0 = -8x_C^3. \end{aligned} \tag{12}$$

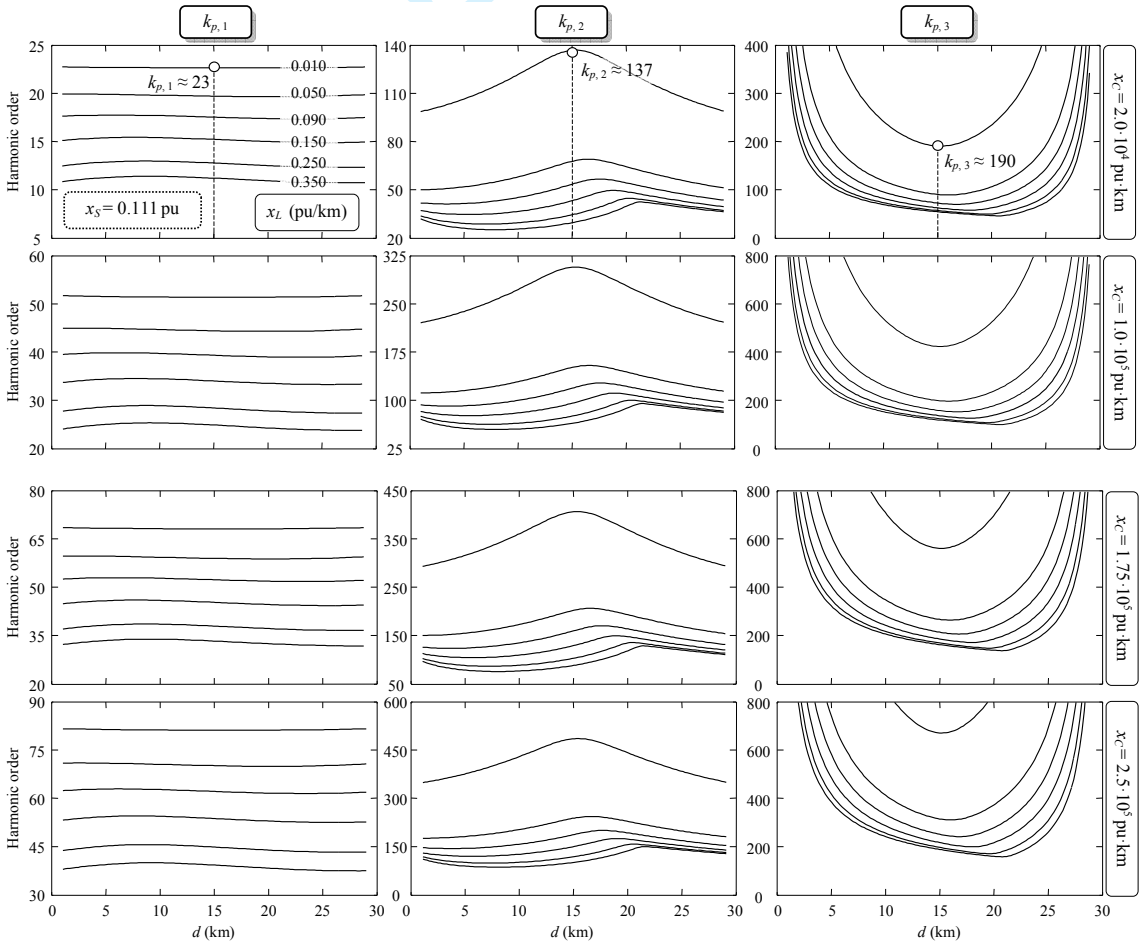

Fig. 3 *Location of the traction system resonances as a function of traction system ratios and train position along a contact feeder section of length D = 30 km.*

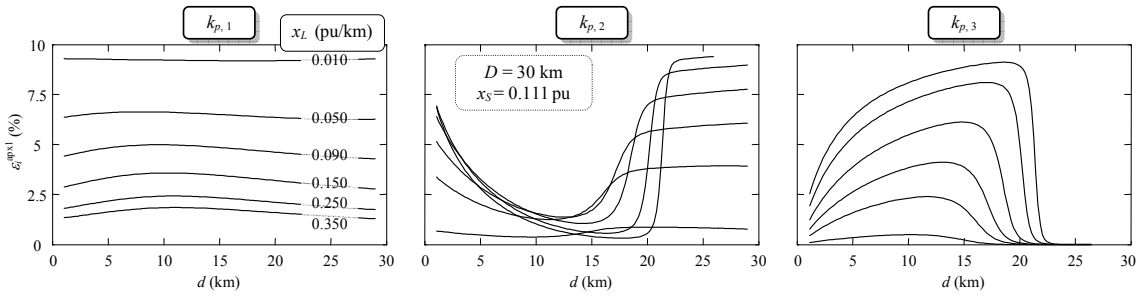

Fig. 4 *Errors in the location of resonances along a contact feeder section of length D = 30 km when the power system reactance X_S (17) is neglected.*

In equation (12), resistance R_L (i.e., ratio r_L) is neglected to reduce the number of variables involved because it is proved that, as expected, it damps the system harmonic response but does not affect resonance location significantly [18]. It is numerically verified that the discriminant of the function in (11),

$$\Delta = 18c_3c_2c_1c_0 - 4c_2^3c_0 + c_2^2c_1^2 - 4c_3c_1^2 - 27c_3^2c_0^2, \tag{13}$$

is greater than zero for the usual track length, all train positions and the ratio range in Table 1.Thus, the solution of the polynomial function corresponds to three real roots, i.e., (14), which allow locating the three parallel resonances in Fig. 2:

$$k_{p,1} = \sqrt{(\alpha - \beta - 2\gamma)} \quad k_{p,2} = \sqrt{\left(\alpha + \frac{\beta}{2}\left(1 + i\sqrt{3}\right) + \left(1 - i\sqrt{3}\right)\gamma\right)} \quad k_{p,3} = \sqrt{\left(\alpha + \frac{\beta}{2}\left(1 - i\sqrt{3}\right) + \left(1 + i\sqrt{3}\right)\gamma\right)}$$
$$\alpha = \frac{-c_2}{3c_3} \qquad \beta = \frac{C}{3c_3} \qquad \gamma = \frac{\left(c_2^2 - 3c_3c_1\right)}{6c_3C}, \tag{14}$$

where

$$C = \left(\frac{1}{2}\left(Q + 2c_2^3 - 9c_3c_2c_1 + 27c_3^2c_0\right)\right)^{1/3} \qquad Q = \sqrt{\left(2c_2^3 - 9c_3c_2c_1 + 27c_3^2c_0\right)^2 - 4\left(c_2^2 - 3c_3c_1\right)^3}. \tag{15}$$

Fig. 3 shows the location of the parallel resonances $k_{p,1}$, $k_{p,2}$ and $k_{p,3}$ as a function of train position d along the contact feeder section of length $D = 30$ km with the ratio range in Table 1. They are calculated from (14) considering six values of ratio x_L ($x_L = 0.01$, 0.05, 0.09, 0.15, 0.25 and 0.35 pu/km), four values of ratio x_C ($x_C = 2.0 \cdot 10^4$, $1.0 \cdot 10^5$, $1.75 \cdot 10^5$ and $2.5 \cdot 10^5$ pu·km) and a single value of ratio x_S ($x_S = 0.111$ pu). Similar curves are obtained for the other values of ratio x_S in the range of Table 1. This ratio has a negligible influence on the resonance because its values, derived from the typically large values of system short-circuit power S_S (1), are very small [2]. The resonances in the example of Section 3 ($D = 30$ km, $d = 15$ km, $x_s = 0.111$ pu, $r_L = 0.003712$ pu/km, $x_L = 0.01$ pu/km and $x_C = 2.0 \cdot 10^4$ pu·km) are also shown in Fig. 3 to verify the usefulness of (14) in locating the resonances despite neglecting the longitudinal resistance of the section line. Note that the low-order harmonics at which the parallel resonances occur are found for higher ratios x_L and lower ratios x_C. The first parallel resonance ($k_{p,1}$), which does not depend on the train position, could be close to the harmonics of the currents injected by train converters (i.e., below the 40th harmonic order) for most values of ratios x_L and x_C. This is not true for the other two resonances but $k_{p,2}$ could also occur below the 40th harmonic

order for x_L greater than 0.1 pu/km and x_C smaller than $5 \cdot 10^4$ pu·km. The analysis of the effect of feeder section length D on the location of the first resonance $k_{p,1}$ from (14) results in the plot $k_{p,1}$ vs D in [7]. It is concluded that the frequency of the resonance is reduced with section line length, but for lengths greater than 40 the influence on resonance location is insignificant. Thus, one design suggestion would be to use the shortest possible sections so that resonance is shifted to higher values.

Although it is easy to locate parallel resonances from the coefficients in (12) using current software tools, simpler expressions of the polynomial function coefficients can be derived by neglecting the short-circuit reactance X_S, i.e., $x_S = X_S/X_{TR} \approx 0$:

$$c_3 \approx x_L^2 D \cdot d^2 \cdot (D-d)^2 \qquad c_2 \approx -2x_C x_L D \cdot \left(\left(D^2 - D \cdot d + d^2 \right) + x_L d \cdot (D-d)^2 \right)$$
$$c_1 \approx 4x_C^2 D \cdot \left(2 + D \cdot x_L \right) \qquad c_0 = -8x_C^3, \tag{16}$$

This makes it possible to obtain friendlier expressions (referred to as $k_{p,i}^{\text{apx1}}$ with $i = 1, 2$ and 3) to locate approximately the harmonics at which parallel resonances occur. To illustrate the goodness of the above approximation, Fig. 4 shows the error between $k_{p,i}$ and $k_{p,i}^{\text{apx1}}$ expressions of the three parallel resonances ($i = 1$, 2 and 3) as a function of the train position along the contact feeder section of length 30 km and considering six values of ratio x_L ($x_L = 0.01$, 0.05, 0.09, 0.15, 0.25 and 0.35 pu/km), any value of ratio x_C (the errors are independent of this ratio) and a single value of ratio x_S ($x_S = 0.111$). This error is evaluated as

$$\varepsilon_i^{\text{apx}j} = \frac{k_{p,i} - k_{p,i}^{\text{apx}j}}{k_{p,i}} \qquad (i = 1,2,3 \quad ; \quad j = 1). \tag{17}$$

It must be noted that the maximum error is always below 10 %. This error is smaller for lower values of ratio x_S. As an example of the above study, Fig. 5(a) compares the results of $k_{p,1}$ and $k_{p,1}^{\text{apx1}}$ as functions of train position d along the contact feeder section of length 30 km and for $x_S = 0.111$ pu, $x_C = 2.0 \cdot 10^4$ pu·km and six values of x_L ($x_L = 0.01$, 0.05, 0.09, 0.15, 0.25 and 0.35 pu/km). The resonances in the example of Section 3 ($D = 30$ km, $d = 15$ km, $x_s = 0.111$ pu, $r_L = 0.003712$ pu/km, $x_L = 0.01$ pu/km and $x_C = 2.0 \cdot 10^4$ pu·km) are also shown in Fig. 5(a) for comparison purposes.

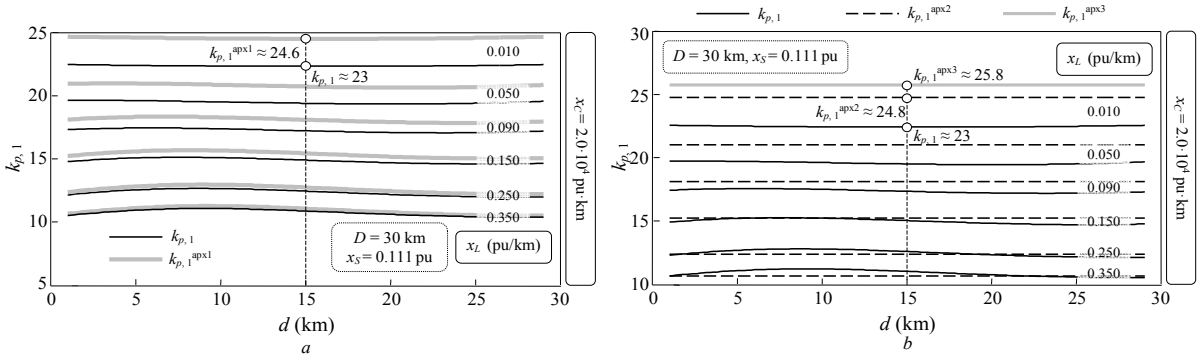

Fig. 5 *First resonance location along a contact feeder section of length D = 30 km*
a Accuracy study of the first approximation, $k_{p,1}^{\text{apx1}}$ [(14) with coefficients in (16)]
b Accuracy study of the second and third approximations, $k_{p,1}^{\text{apx2}}$ (20) and $k_{p,1}^{\text{apx3}}$ (21)

4.3 Study of the first parallel resonance

Although the three parallel resonances determined in (14) and shown in Fig. 3 are reported in the literature, only the first (i.e., the $k_{p,1}$ resonance) is studied because of its proximity to the switching frequency of train converters. This Section analyzes the dependence of this resonance on traction system parameters. Moreover, two approximate expressions to locate the resonance are proposed and their accuracy and limitations are discussed.

By considering the approximations of the longitudinal resistance of the section line and the short-circuit reactance of the power system in the previous Section, and the slight dependence of $k_{p,1}$ (i.e., first resonance) on train position d (see Figs. 4 and 5(a)) [2], [4], [7], [14], [15], this resonance can be approximately located by imposing $R_L \approx 0$ and $X_S \approx 0$ and setting any value of d in the admittance expressions (6). That is, harmonic $k_{p,1}$, at which the first resonance occurs, can be roughly determined by neglecting the section line resistance and the power supply reactance in the circuit of Fig. 1(b) and placing the train at the beginning of the contact feeder section (i.e., $d = 0$ km). As can be seen in the resulting circuit, the expression of the normalized equivalent impedance at the load terminals is

$$\underline{Z}_{Eqk,N}^{\text{apx}2} = \frac{\underline{Z}_{Eqk}^{\text{apx}2}}{X_{TR}} = \frac{1}{X_{TR}} \frac{1}{\underline{Y}_{Eqk}^{\text{apx}2}} = \frac{1}{X_{TR}} j \left(\frac{1}{kX_{TR}} - \frac{D \cdot k}{2X_C} + \frac{1}{\left(kX_L D - \frac{2X_C}{D \cdot k} \right)} \right)^{-1}, \tag{18}$$

and the first resonance of $\underline{Z}_{Eqk,N}$ can be approximately located by equating to zero the denominator of (18), which can be compacted as follows:

$$\text{Den}\left(\underline{Z}_{Eqk,N}^{\text{apx}2} \right) = x_L D^3 \cdot k^4 - 2x_C D \cdot (D \cdot x_L + 2) \cdot k^2 + 4x_C^2. \tag{19}$$

Thus, the first parallel resonance in (14) ($k_{p,1}$) can be approximated by the following root of equation (20):

$$k_{p,1}^{\text{apx}2} = \frac{1}{D} \sqrt{\frac{x_C}{x_L} \left(D \cdot x_L + 2 - \sqrt{D^2 \cdot x_L^2 + 4} \right)}. \tag{20}$$

To illustrate the usefulness of the above approximation, Fig. 5(b) compares the results from

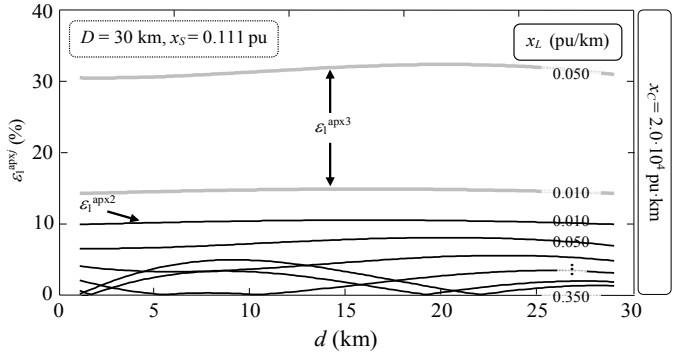

Fig. 6 *Errors in the first resonance location with $k_{p,1}^{apx2}$ (20) and $k_{p,1}^{apx3}$ (21).*

expressions $k_{p,1}$ (14) and $k_{p,1}^{apx2}$ (20) and Fig. 6 shows the error ε_1^{apx2} (17) between them as a function of the train position d along the contact feeder section and for $D = 30$ km, $x_S = 0.111$ pu, $x_C = 2.0 \cdot 10^4$ pu·km and six values of x_L ($x_L = 0.01$, 0.05, 0.09, 0.15, 0.25 and 0.35 pu/km). The resonances in the example of Section 3 ($D = 30$ km, $d = 15$ km, $x_s = 0.111$ pu, $r_L = 0.003712$ pu/km, $x_L = 0.01$ pu/km and $x_C = 2.0 \cdot 10^4$ pu·km) are also shown in Fig. 5(b) for comparison purposes. Note that the excellent accuracy of the approximation (with errors below 10%) can be extended to the other values of the traction system parameters in Table 1.

It can be observed that for $D^2 \cdot x_L^2 << 4$ (i.e., if the longitudinal reactance X_L of the catenary is small enough), the $k_{p,1}^{apx2}$ expression in (20) can be simplified as

$$k_{p,1}^{apx3} = \sqrt{\frac{x_C}{D}} = \sqrt{\frac{1}{D}\frac{X_C}{X_{TR}}}. \tag{21}$$

This expression can also be deduced by neglecting the section line resistance R_L, the power supply reactance X_S, and the longitudinal reactance X_L in the circuit of Fig. 1(b), and equating to zero the denominator of the normalized equivalent impedance at the train terminals when the train is located at the beginning of the contact feeder section (i.e., $d = 0$ km):

$$\underline{Z}_{Eqk,N}^{apx3} = \frac{\underline{Z}_{Eqk}^{apx3}}{X_{TR}} = \frac{1}{X_{TR}}\frac{1}{\underline{Y}_{Eqk}^{apx3}} = \frac{1}{X_{TR}} j\left(\frac{1}{kX_{TR}} - \frac{D \cdot k}{X_C}\right)^{-1}. \tag{22}$$

The above approximation is commonly used in traction system studies assuming that the first parallel resonance is independent of the train position along the section line [2], [4], [7], [14], [15] and is mainly determined by the substation reactance X_{TR} and the per-unit-length capacitive reactance X_C between the contact wire and the ground [2], [7]. However, in the authors' knowledge, its application range has been neither theoretically justified nor limited. To illustrate this assertion, Fig. 5(b) compares the results from expressions $k_{p,1}$ (14) and $k_{p,1}^{apx3}$ (21) and Fig. 6 shows the error ε_1^{apx3} (17) between them as a function of the train position d along the contact feeder section and for $D = 30$ km, $x_S = 0.111$ pu, $x_C = 2.0 \cdot 10^4$ pu·km and six values of x_L ($x_L = 0.01$, 0.05, 0.09, 0.15, 0.25 and 0.35 pu/km). Note that, as $k_{p,1}^{apx3}$ is independent of x_L, it is plotted as a single line which moves further away from $k_{p,1}$ with increasing the longitudinal reactance of the section line (i.e., ratio x_L). Thus, $k_{p,1}^{apx3}$ gives an acceptable error (close to 10 %) only for values x_L below 0.01 pu/km. Above this value, the error increases dramatically, invalidating the approximation. This is also true for the other values of the parameters in Table 1.

5 Application of harmonic resonance location

The analytical expressions of $k_{p,1}$ [(14) with coefficients in (12)], $k_{p,1}^{apx1}$ [(14) with coefficients in (16)], $k_{p,1}^{apx2}$ (20) and $k_{p,1}^{apx3}$ (21) are applied to locate the harmonic resonance of three 1x25kV 50Hz traction power systems in the literature, [3], [15], [16].

Table 2 *1x25kV 50 Hz traction systems in the literature*

REFERENCE			[3]	[15]	[16]
SUBSTATION TRANSFORMER	Reactance	X_{TR} [Ω]	7.2257	8.5137	4.7124
CONTACT FEEDER SECTION	Long. π- resistance	R_L [Ω/km]	0.200	0.169	0.15
	Long. π-reactance	X_L [Ω/km]	0.4492	0.4335	0.3142
	Transv. π-reactance	X_C [Ω·km]	$1.55 \cdot 10^5$	$2.89 \cdot 10^5$	$2.12 \cdot 10^5$
	Track length	D	40	30	30
	Train position	d	20	10	30
RESONANCE	1st	$k_{p,1}^{[Ref]}$	≈ 16	≈ 26	≈ 28
		$k_{p,1} \approx k_{px1,1}^{a}$	16.02	27.30	29.46
		$k_{p,1}^{apx2}$	16.72	27.36	29.63
		$k_{p,1}^{apx3}$	23.17	33.65	38.72
	2nd	$k_{p,2}^{[Ref]}$	≈ 49	≈ 90	≈ 70
		$k_{p,2} \approx k_{px1,2}^{a}$	49.41	74.75	69.50
	3rd	$k_{p,3}^{[Ref]}$	---	---	---
		$k_{p,3} \approx k_{px1,3}^{a}$	65.45	151.34	599.96

Note: "--- " means that no data are available.

In [3], a harmonic study on the Velesin (Czech Republic) traction system is presented. The voltage and current at the traction substation are measured and compared with Microcap simulation results by programming the equivalent circuit model with the electrical parameters of the traction system. The voltage and current waveforms reveal the presence of resonances in the traction system, which are analyzed from equivalent circuit simulations.

In [15], the performance of a hybrid shunt compensation system connected at one end of a traction feeder section is studied by simulation and experiments to address the resonance phenomena. The study considers typical 1x25 kV 50 Hz traction substations with 30 km single-phase contact feeder sections and provides their electrical parameters.

In [16], technical details of several traction systems such as harmonic distortion, resonance phenomena and AC filters are analyzed from their electrical specifications.

Table 2 summarizes the traction system electrical parameter data provided by the above references and the harmonic orders at which the parallel resonances are located. The lack of information on the short-circuit power of the supply networks is not a problem because of its small influence on the resonances (see $k_{p,1}^{apx1}$ errors in Fig. 5). Thus, a 700 MVA value is assumed. With these data, a harmonic study on parallel resonance location is performed from the analytical expressions in Section 4. Results are reported in Table 2, together with the results in the references. It must be noted that the results of expressions $k_{p,i}$ and $k_{p,i}^{apx1}$ ($i = 1, 2$) are in agreement with those in the original works. In the case of [15], the result of $k_{p,2}^{apx1}$ does not exactly agree with $k_{p,2}^{[Ref]}$, probably due to differences in the modeling of the section line. These have no effect on the location of the first resonance but they do on the location of the other resonances. Expression $k_{p,1}^{apx2}$ also gives correct

results, unlike expression $k_{p,1}^{apx3}$, whose results are unacceptable because the longitudinal reactance of the contact feeder section is too large compared to the substation transformer reactance ($x_L > 0.01$ pu/km in the three examples).

6 Conclusions

Train converters are non-linear loads that inject harmonic currents at pantograph terminals capable of causing voltage waveform distortion. This problem can be magnified by the parallel resonance of the equivalent impedance observed from the traction load. In unfiltered traction systems, this impedance has three parallel resonances but only that below 2 kHz can be really dangerous because of its proximity to the frequency of harmonic currents injected by converters. This paper contributes to locating the harmonics at which the three parallel resonances occur by providing analytical expressions. Using these expressions and considering system electrical parameters, it is possible to analyze the resonance frequencies in more detail than frequency scan plots. The study of the lowest parallel resonance shows that this resonance hardly depends on train position, allowing the derivation of a simpler expression to locate it. Moreover, if the longitudinal reactance of the section line is 0.01 times smaller than the substation transformer reactance, the previous expression can be further simplified and the harmonic of the parallel resonance is mainly dependent on the substation reactance, the per-unit-length capacitive reactance between the contact wire and the ground and the contact feeder section length. This approximation is commonly used in the literature without considering its application range. The proposed expressions are validated by analyzing the frequency response of several traction systems in the literature.

7 References

1 Dolara, A., Gualdoni, M., Leva, S. "Impact of high-voltage primary supply lines in the 2x25 kV – 50 Hz railway system on the equivalent impedance at pantograph terminals", *IEEE Trans. on Power Delivery*, Vol. 27, No. 1, pp. 164-175, 2012.

2 Janssen, M. F. P., Gonçalves, P. G., Santo, R. P., Smulders, H. W. M., "Simulations and measurements on electrical resonances on the Portuguese 25 kV network", *Proceedings of the World Congress on Railway Research*, pp. 18-22, 2008.

3 Kolar, V. et al., "Interference between electric traction supply network and distribution power network – Resonance phenomenon", *Proceedings of the 14th IEEE Int. Conference on Harmonics and Quality of Power*, pp. 1-4, 2010.

4 Kumar S. R. et al, "Harmonic levels in a traction system - An overview", *Proceedings of the Power Quality*, pp.139-143, 1998.

5 Griffin, A. J., "Methods of improving the voltage regulation on 25kV electric railways", *Proceedings of the Int. Conference on Main Line Railway Electrification*, pp.252-259, 1989.

6 Aeberhard, M., Courtois, C., Ladoux, P., "Railway Traction Power Supply from the state of the art to future trends" *Proceedings of the Int. Symposium on Power Electronics, Electrical Drives, Automation and Motion (SPEEDAM)*, pp. 1350–1355, 2010.

7 Brenna, M. et al, "Investigation of resonance phenomena in high speed railway supply systems: Theoretical and experimental analysis", *Electric Power Systems Research*, Vol. 81, No. 10, pp. 1915-1923, 2011.

8 Hill, R. J. "Electric railway traction. Part3: Traction power supplies', *Power Eng. Journal*, Vol. 8, pp. 275-286, 1994.

9 Capasso, A. et al, "Harmonics and PQ events monitoring in an electrified metro-transit system", *Proceedings of the Int. Conference on Harmonics and Quality of Power (ICHQP),* vol. 2, pp. 441-446, 2002.

10 Caramia, P., Morrone, M., Varilone, P., Verde, P. "Interaction between Supply System and EMU Loco in 15kV-16 2/3 Hz AC Traction Systems", *Proceedings of the Power Society Summer Meeting*, pp. 198-203, 2001.

11 Hamoud, O., "Harmonic problems in Queensland railway electric traction system", *Proceedings of the Int. Conference on Main Line Railway Electrification*, pp. 227–231, 1989.

12 Holtz, J., Klein, H-J. "The Propagation of Harmonic Currents Generated by Inverter-Fed Locomotives", *IEEE Trans. on Power Electronics*, Vol. 4, Num. 2, pp. 168-174, 1989.

13 Tan, P-C., Chiang, P., Grahame, D. "Optimal Impedance Termination of 25-kV Electrified Railway Systems for Improved Power Quality", *IEEE Trans. on Power Delivery*, Vol. 20, Num. 2, pp. 1703-1710, 2005.

14 Guo, L., Li, Q., Xu, Y., "Study on harmonic resonance of traction line in electrified high-speed traction system", *Proceedings of the Int. Conference on Sustainable Power Generation and Supply (SUPERGEN)*, pp. 1-4, 2009.

15 Tan, P-C., Chiang, P., Grahame, D. "A robust multilevel hybrid compensation system for 5-kV electrified railway applications", *IEEE Trans. on Power Delivery*, Vol. 19, Num. 4, pp. 1043-1052, 2004.

16 Buhrkall, L., "Traction system case study", *Proceedings of the IET Professional Development course on Electric Traction Systems*, pp.45-63, 2008.

17 Kiss, P., Dán, A., "The application of the double domain simulation by different harmonic filtering methods of 25 kV electric traction systems", *Proceedings of the 13th IEEE Int. Conference on Harmonics and Quality of Power*, pp. 1-6, 2008.

18 Sainz, L., Monjo, L., Riera, S., Pedra, J. "Study of Steinmetz circuit influence on AC traction system resonance", *IEEE Trans. on Power Delivery*, Vol. 27, Num. 4, pp. 2295-2303, 2012.